# Assessment of Urban Heat Island in Abuja Municipal Area Council FCT-Abuja

[1]Danbaba Goma and [2]Yahaya Ishaya Kuku

[1]Department of Environmental Management, Faculty of Environmental sciences, Bingham University, Kodape-Karu, Nigeria
[2]Department of Geography, Nigerian Army College of Education Ilorin, Kwara State.
Email: danbaba.goma@binghamuni.edu.ng & ishaya.yahaya@army.mil.ng

## Abstract

Cities around the world are being faced with an undesirable increase in air temperature. This is indicated by an increase in non-porous, non-evaporating, highly thermal conductive surfaces which has replaced the vegetation biomass resulting to the formation of Urban Heat Island (UHI). This study employed geo-spatial techniques to determine UHI intensity in Abuja Municipal Area Council (AMAC). The Landsat images used were acquired from United States Geological Survey (USGS) for the period of 2003, 2013 and 2023. Supervised image classification using the maximum like-hood algorithm was utilised. The classifications were based on a +3°C temperature rise within a range depiction of UHI intensity across the study area, categorized into five distinct temperature ranges. The results obtained reveal that Land Surface Temperature (LST) for 2003 is within the ranges of 28° - 31°C and 31° - 34°C covering 52.77% and 36.75% of the total study area respectively. From 2013 and 2023; surface temperature within the range of 28º to 34ºC was seen to dominate the spatial extent of the study area. In 2003, 2013 and 2023 the northern part of the study area exhibits moderate to high UHI intensities. On the other hand, the southern outskirts show lower UHI intensities. The highest UHI intensities range from 0.62 to 0.975°C and the moderate UHI intensity range from 0.391 to 0.619 °C. In order to reduce the occurrence of UHI in the study area, the study recommended sustainable urban development and increasing plant cover.

**Keywords:** urban heat island, satellite remote sensing, air temperature, Abuja Municipal.

## Introduction

Urbanization is a major event in human history and there is no doubt the world is urbanizing rapidly at present. According to the United Nation Development Programme (2022), approximately 2% of the earth's land surface is covered by urban regions which contain about half of the human population. The global human population in urban centres have been increasing at various percentage of the entire global population. It was projected that by 2030, 60% of the world's population will live in urban areas and increase to approximately 70% by 2050 (World Urbanization Prospects, 2019; Ashley, 2016).

According to Mande and Abashiya (2020), globally urbanization and human activities are known to be the major determinants inducing changes to the physical characteristics of the earth as well as changes in the urban microclimate. In most large cities, urbanization always takes place at the city core and sprawl to its fringes which make the temperature at the heart of the city's central business district (CBD) to be higher than its surroundings or the suburban area (Agu *et al*, 2021). The process of urbanization can increase local temperature in comparison to less built up suburban/rural areas, creating an UHI (Mande & Abashiya, 2020). The term "UHI" refers to the observed temperature difference between urban environments and the surrounding rural areas

(Alfraihat *et al,* 2016). Observations have shown that the temperatures of urban centres can be up to 12°C higher than neighbouring regions (Alfraihat *et al,* 2016). UHI can be defined as the, relative warmth of a city compared to the surrounding rural areas, which is relatively cool (Agu *et al,* 2021).

The concept of UHI was first investigated and described by Howard in London. In 1815, Howard conducted the first-ever systematic urban climate study, measuring what is now called the UHI effect based on thermometers in the city of London and the countryside nearby (Ashley, 2016). Howard stated that "An UHI refers to any area, populated or not which is consistently hotter than the surrounding area'. UHI is also referred to the elevated temperatures in built-up areas compared to rural surroundings. 'UHI effect on the other hand means the atmospheric temperature rise experienced by any urbanized area (Nguyen *et al,* 2018; Meenal & Rajashree, 2017). About UHI intensity, it does not only vary between cities but also vary within cities.

Several studies on UHI such as Adinna *et al* (2009), Khaled *et al* (2015), Archisman (2017), Adebayo *et al* (2017), Ayalade *et al* (2021), Ammar (2021), Agu *et al* (2021) have been conducted in so many parts of the world. Findings from these studies provided a ground to state that land cover change accelerated by human activities brings about an increase in heat-related illnesses and deuteriation of living environment; increase energy consumption and elevation of ground-level ozone and induce urban air quality due to heat waves (Ayalade *et al,* 2021). In the same way, urban local climate can also be affected. Also, it was found that heat-related mortality is higher in cities than in suburbs and that a 3°C increase may cause an increase in hospital admissions (Aghamohammadi *et al,* 2021).

Abuja, being the Federal Capital Territory of Nigeria, is not an exception to this observed Land Use Land Cover (LULC) changes. Analysis of Land Use Land Cover (LULC) in Abuja Municipal Area Council (AMAC) of Nigeria showed increasing trend in urban growth and change in land cover (Nkeki & Ojeh, 2014). The causes of the rapid growth of Abuja have been a major concern to researchers. Essentially, the two causes mostly referred to in literatures have been the continued rural-urban migration and the rate of natural increase (Muhammad, Abubakar & Shehu, 2013). Thomas (2020), Isioye *et al* (2020) and Awuh *et al* (2021) reported separately, that another significant effect of this urban expansion is the variation in Land Surface Temperature (LST). LST means the skin temperature of the land surface and is one of the important parameters in urban climate as it serves as an indicator for measuring UHI. It has a significant influence on air temperature, especially the canopy layer that is closest to the surface (Awuh *et al,* 2021). Furthermore, the replacement of the vegetation and other natural surfaces by unnatural or man-made materials like asphalt, concrete, metal, in urban areas have environmental implications that include reduction in evapotranspiration, rapid run-off and increase in surface temperatures leading to creation of UHI (Thomas, 2020; Isioye *et al,* 2020).

This indicates a likely relationship between urban growth, LST and UHI in Nigeria. This has necessitated the aim of this study, which is to assess UHI effects on the surface temperature of Abuja Municipal Area Council (AMAC).

## Description of the Study Area

Abuja Municipal Area Council (AMAC) is located in the east of Federal Capital Territory, Abuja. It lies between latitudes 7˚49" and 8˚49" north of the equator, and longitudes 7˚07" and 7˚33" east of the Greenwich Meridian (Fig. 1). Also, AMAC is the largest and most developed of the six area councils in the FCT as evidenced by its landmass of approximately 2,500km² (Balugun, 2001). The study area is topographically characterized by a blend of hilly and levelled land surface. This is demonstrated by numerous hills and rocks especially in Jahi, Maitama, Asokoro, Wuye and Apo, while other areas are characterized by slopes such as Gwarinpa, and others. Like every other location in Abuja, the study area is composed of hot, humid, and tropical climatic condition and it falls within the guinea savanna ecological zone with its main vegetation being categorized into grass, woodland, and shrub (Adakayi, 2000). The general increasing human population and urban sprawl in the FCT Abuja results in the emergence of satellite towns and smaller settlements. Consequently, there has been a corresponding loss of vegetation which exerts a substantial influence on the micro-climate of the area (Adakayi, 2000).

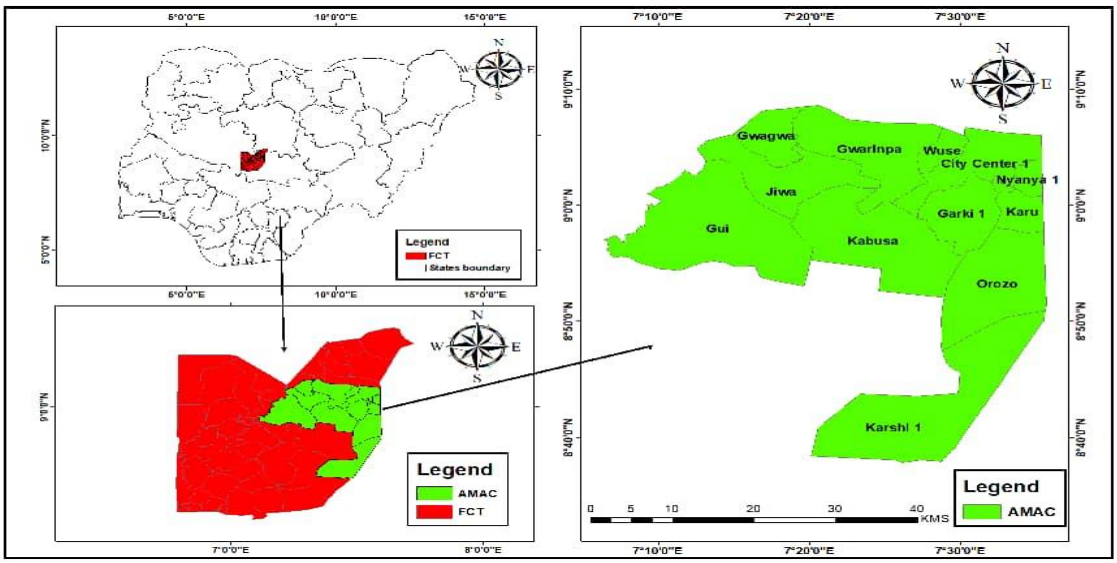


**Figure 1: Study area (AMAC LGA)**

## Materials and Methods

### Data Collection

Various spatial analyses were performed for AMAC. of which, Landsat 8 operational land imager (OLI) and 7 thematic mapper (TM) data were obtained from United States Geological Survey - USGS- Earth Explorer (www.usgs.gov) and was downloaded at the epochs of November, March and April (i.e., to get the best cloud free image); 2003, 2013 and 2023. For the analysis, aster's digital elevation model was also downloaded and extracted. Information about the satellite images used as sources for this study's analysis is shown in Table 1.

**Table 1: Sourced Satellite Imagery**

| Date of Acquisition | Satellite Data | Sensor | Band No. | Spectral range (Wavelength $\mu$m) | Spatial Resolution (m) |
|---|---|---|---|---|---|
| 21/11/2003 | Landsat 7 | TM | 1 | 0.45–0.52 | 30 |
| | | | 2 | 0.52–0.60 | 30 |
| | | | 3 | 0.63–0.69 | 30 |
| | | | 4 | 0.76–0.90 | 30 |
| | | | 6 | 10.4012.50 | 120 resampled to 30 |
| 16/03/2013 | Landsat 7 | TM | 1 | 0.45–0.52 | 30 |
| | | | 2 | 0.52–0.60 | 30 |
| | | | 3 | 0.63–0.69 | 30 |
| | | | 4 | 0.76–0.90 | 30 |
| | | | 5 | 1.551.75 | 30 |
| | | | 6 | 10.4012.50 | 120 resampled to 30 |
| 05/04/2023 | Landsat 8 | OLI | 2 | 0.45–0.51 | 30 |
| | | | 3 | 0.64–0.67 | 30 |
| | | | 4 | 0.53–0.59 | 30 |
| | | | 5 | 0.85–0.88 | 30 |
| | | | 6 | 1.57–1.65 | 30 |
| | | TRIS 1 | 10 | 10.60–11.19 | 100 resampled to 30 |
| | | TRIS 2 | 11 | 11.50–12.51 | 100 resampled to 30 |
| 10/04/2023 | DEM | SRTM | --- | --- | 1 Arc |

Source: Modified from Landsat Imageries, 2024

**Image Pre-processing and Analysis**

Datasets were masked using the clip boundary function of ESRI's ArcGIS 10.2.2 software for AMAC. Atmospheric and Radiometric corrections were carried out on both Landsat 7 and 8 which were the downloaded satellite imagery. Scan line error correction was also performed on Landsat 7 TM imagery obtained to enhance resolution for analysis. Satellite images obtained were combined and True Color Composite (TCC) was created using appropriate band combinations for all images to enable the creation of training samples and identify the various LULC classes (Good & Giordano, 2019). Maximum Likelihood Supervised Classification (MLSC) approach was used to categorize Landsat Images into four major LULC classes for the years 2003, 2013 and 2023. For each LULC class, a total of 30 samples were collected to create LULC maps. Each categorized map has been assessed for accuracy using user and producer accuracy, and kappa index (Pontius & Millones, 2011). Based on the fact that the National Aeronautics and Space Administration's (NASA) ASTER Global Digital Elevation Map (version 2) had a spatial resolution of 30m by 30m,

elevation data was made available. To get a working spatial resolution of 100m x 100m, the dataset was resampled. Additionally, the slope map was created using these elevation data.

**Land Surface Temperature (LST)**

i. Conversion to Top Atmosphere (TOA) Radiance: using the radiance rescaling factor, Thermal infra-red digital numbers were converted to TOA spectral radiance using equation 1a for Landsat 7 TM data and 1b for Landsat 8 OLI data (Liu & Zhang, 2011).

$$L\lambda = \left(\frac{(Lmax - Lmin)}{(QCALmax - QCALmin)}\right) \times (QCAL - QCALmin) + Lmin\lambda \quad - \quad - \quad \text{- (1a) \_Landsat 7 TM}$$

$$L\lambda = ML \times Qcal + AL \quad - \quad - \quad - \quad \text{- (1b) \_Landsat 8 OLI}$$

Where:
$L\lambda$ = TOA spectral radiance (Watts / ($m^2$ * sr * $\mu$m)
$ML$ = Radiance Multiplicative Band
$AL$ = Radiance Add Band
$Qcal$ = Quantized and calibrated standard product pixel values

$O_i$ = Correction value for Band 10 is 0.29

ii. Conversion to Top of Atmosphere (TOA) Brightness Temperature (BT): Utilising the thermal constant values from the downloaded Landsat metadata file, the spectrum of the thermal infrared band was converted to active radiance sensor brightness temperature. $-273.15$ which was added to the equation to enable temperature unit conversion from Kelvin (K) to Celsius Degrees (℃) (Rahman *et al*, 2017; Sholihah & Shibata, 2019).

$$BT = \left(\frac{K2}{\ln\left({}^{K1}/_{L\lambda}\right)} + 1\right) - 273.15 \quad - \quad - \quad - \quad \text{- (2) \_Landsat 7 \& 8}$$

Where:
$BT$ = Top of Atmosphere temperature
$L\lambda$ = TOA spectral radiance (Watts / ($m^2$ * sr * $\mu$m)
$K1$ = K1 constant Band

$K2$ = K2 Constant Band

The value of K1 and K2 for Landsat 7 and Landsat 8 are given as shown in Table 2 (Liu & Zhang, 2011).

**Table 2: Calibration Constants for Landsat Thermal Bands**

| Constant | Unit K1: W/(m$^2$×sr×μm) | Unit K2: Kelvin |
|---|---|---|
| **Landsat 7 TM** | 666.09 | 1282.71 |
| **Landsat 8 OLI TRIS (Band 10)** | 774.8853 | 1221.0789 |
| **Landsat 8 OLI TRIS (Band 11)** | 480.8883 | 1201.1442 |

Source: Researcher's Compilation, 2024

iii. Normalized Difference Vegetation Indices (NDVI): The Normalized Differential Vegetation Index (NDVI) is a standard vegetation index which is calculated using Near Infra-red and Red respectively. Several scholars have confirmed that the surface emissivity is highly correlated with the NDVI, and so the emissivity can be calculated using the NDVI (Ahmed *et al*, 2013). See equation (3).

$$NDVI = \frac{NIR-RED}{NIR+RED} \quad - \quad - \quad - \quad \text{- (3) \_Landsat 8 OLI}$$

Where:
*RED* = DN Values from the RED Band
*NIR* = DN Values from the Near Infra-red band

Vi. Land Surface Emissivity (LSE): The average emissivity of a component of the earth's surface is measured as land surface emissivity (LSE), which is derived from NDVI data. The aforementioned correction can be achieved by calculating the land surface spectral emissivity (Ɛ). Meanwhile, some elements such as water content, chemical composition, structure, and roughness all affect the emissivity of the surface (Zine-El -Abidine *et al.*, 2014). See equation (4 and 5).

$$PV = \left(\frac{NDVI-NDVI_{min}}{NDVI_{max}-NDVI_{min}}\right)^2 \quad - \quad - \quad - \quad \text{- (4) \_Landsat 8 OLI}$$

Where:
*PV* = Proportion of Vegetation
*NDVI* = DN values from NDVI Image
$NDVI_{min}$ = Minimum DN value from NDVI image
$NDVI_{max}$ = Maximum DN value from NDVI image

$$Ɛ = 0.004 \times PV + 0.986 \quad - \quad - \quad - \quad \text{- (5) \_Landsat 8 OLI}$$

Where:
Ɛ = Land Surface Emissivity
*PV* = Land Surface Vegetation
*0.986* corresponds to a correction value of the equation

v. Land Surface Temperature: The LST is the radiative temperature which was calculated using Top of Atmosphere brightness temperature, wavelength of emitted radiance, Land Surface Emissivity via the following equation 6 (Zine-El-Abidine *et al*., 2014).

$$LST = \frac{BT}{\left(1+\lambda\times\left(\frac{BT}{C_2}\right)\times\ln(E)\right)} \quad - \quad - \quad - \quad -(6)\ \_\text{Landsat 8 OLI}$$

Here, $C_2$ = 143888 um k or 14380

Where:

*BT* = Top of atmosphere brightness temperature (Centigrade C)
$\lambda$ = wavelength of emitted radiance
*E* = Land surface Emissivity
*C2* = $h \times {}^{c}/_{\sigma}$ - - - - - - - - - - - - -(7)
= $1.4388 \times 10^{-2} mk$
= *14388 mk*
*h* = Planck's constant = (6.626 ×$10^{-34}$ Js)
*c* = velocity of light = (2.998 × $10^{8}$ $ms^{-2}$)

$\sigma$ = Boltzmann constant = 5.67×$10^{-8}$ $Wm^2k^{-4}$ = (1.38 × $10^{-23}$ JK)

vi. **Retrieval of Land Surface Temperature (LST) from images brightness**

Land Surface Temperature (LST) was retrieved using a single window algorithm:

LST = TB / 1 + (λ + TB/ ρ) In ε - - - - - - - - - - - - - - - - (8)

Where:
λ = represents the wavelength of the emitted radiance which is equal to 11.5μm.
ρ = represents h.c/σ,
σ =represents Stefan Boltzmann's constant which is equal to 5.67 x 10-8 Wm-2 K -4,
h = represents Plank's constant (6.626 x 10 -34 J S)
c =represents velocity of light (2.998 x 108 m/sec) and

ε = represents spectral emissivity.

All the procedures above (for estimating land surface temperature) were computed using the map algebra function in Spatial

Analyst in ArcGIS 10.2.2 software.

**Results of Findings**

The categorized imagery for 2003 revealed a larger portion of area were occupied by dense vegetation 1114.80km² which represents 42.23% of the total land. In 2013 it decreased to 677.74km² which accounts for 25.67% of the total area and in 2023 it was lowered up to 188.82km² which represents 7.15% of the total area. Low level of urban growth and few other technological activities needed to convert vegetation land to built-up area for human settlement, commercial and other forms of agricultural land usage. This finding is similar to that of Hammad *et al*. (2018) where vegetation area decreased from about 64% in 1987 to about 38% in 2017. In 2003 shrub occupied 913.76km² which represents 34.61% of the total land. The progressive significant

increase continued up till 2013 which occupied 1197.42km² and accounted for 45.36% of the total land but in 2023, it slightly declined to 1110.82km² which constituted 42.07% of the total land area. In 2003 bare land constituted 519.99km$^2$ which accounted for 19.70% and progressively increased from 655.63km$^2$ which represented 24.83% in 2013 to 1102.47km$^2$ which accounted for 41.76% in 2023. In 2003 built area occupied 91.45km$^2$ which represented 3.46% and continue to increase from 109.20km$^2$ which constituted 4.14% in 2013 to 237.89km$^2$ which accounted for 9.01% in 2023 (Table 3).

**Table 3: Change Analysis for LULC in the study area from 2003 to 2023**

| Land Use | Area in km² | | | Change in % | |
|---|---|---|---|---|---|
| | 2003 | 2013 | 2023 | Δ 2003 _ 2013 | Δ 2013 _ 2023 |
| Built-up areas | 91.45 | 109.20 | 237.89 | 0.67 | 4.87 |
| Baren terrain | 519.99 | 655.63 | 1102.47 | 5.14 | 16.93 |
| Shrub land | 913.76 | 1197.42 | 1110.82 | 10.74 | -3.28 |
| Dense Vegetation | 1114.80 | 677.74 | 188.82 | -16.56 | -18.52 |
| Total = | 2,510 | 2,510 | 2.510 | | |

Source: Researcher's Analysis, 2024 **Δ** Percentage Change

An important aspect of change detection is to determine what is actually changing. The major changes that occurred between the periods of 2003 and 2013 were mainly evident in the decrease in dense vegetation. Vegetation loss to other LULC categories was -16.56km². The net rate of change between 2013 and 2023 shows that the different land use types such as dense vegetation and shrub have a negative loss change. Danse vegetation rate of loss is -18.52km² and shrub is -3.28km². It can be noticed during the period under consideration that, dense vegetation and rock shrub LULC lost their land in favour of bare and built land. All these are negative changes that enabled bare-land to gain 16.93km² and built 4.87km² (Table 3). Vegetation land was the most affected and this has implication on the climatic condition in the study area. Comparing the LULC results from 2003, 2013, and 2023 allowed for the calculation of the percentage change in each land cover class over time. The amount of vegetated land declined significantly by 18.53 percent between 2013 and 2023. The built-up area increased by 4.87% of the entire study area during the same time period (Table 3).

Deforestation, urban sprawl, and other human activities like agricultural practises have significantly changed the climatic conditions and fragmented the vegetal cover of the planet. Vegetation provides many ecosystem services, including removing carbon dioxide from the atmosphere, reducing soil erosion, and preventing flooding. Important ecosystem services will be altered or destroyed when forest areas are converted to built-up area. The result also substantiates the finding of Oyinloye (2013) who asserted that the direct relationship between rapid urban growth and commercial centres, industrial centres, tourism resorts and population influx has a basis from land use changes. The reduction in vegetation decreased the amount of oxygen in the air, which worsened the effects of the problem associated to urban heat islands over the study area.

## LULC Accuracy Assessment

30 sampling sites were compared with the equivalent point on Google Earth pictures taken during the same period in order to validate the land use classification. Whereas, the validation, the Kappa coefficient statistics, and the overall classification accuracy all demonstrated good accuracy.

**Table 4: Accuracy Assessment for LULC Classification**

| | 2003 (%) | 2013 (%) | 2023 (%) |
|---|---|---|---|
| Overall Accuracy | 83.33 | 81.31 | 86.67 |
| Kappa Coefficient | 77.74 | 78.38 | 82.20 |

**Source: Researcher's Analysis, 2024.**

The accuracy level is classified as very strong when the Kappa coefficient is greater than 0.75 (Congalton & Green, 2008). Table 4 shows the classification of overall accuracy and the land use classification Kappa coefficient as a result. The total accuracy for the years 2003, 2013, and 2023 was 83.33%, 81.31%, and 86.67%, respectively; the corresponding Kappa coefficients were 77.74%, 78.38%, and 82.20%. The results are in tandem with Kappa coefficient values (above 0.75) which indicate that the LULC data produced by the MLSC procedure has a high enough accuracy to be useful for analyzing LULC and identifying changes (Mondal *et al*, 2016).

## Land Surface Temperature Change/Transition Analysis

The land surface temperature of Abuja metropolis for 2003, 2013 and 2023 is given in Table

**Table 5: Change Analysis for LST in the study area from 2003 to 2023**

| LST Range | Area in km² | | | Change in % | |
|---|---|---|---|---|---|
| | 2003 | 2013 | 2023 | Δ 2003 – 2013 | Δ 2013 – 2023 |
| < 25° | 0.68 | 1.17 | 0.94 | -0.013 | -0.008 |
| 25 - 28° | 215.35 | 228.87 | 51.84 | 0.499 | -6.142 |
| 28 - 31° | 1521.33 | 1656.7 | 308.58 | 4.696 | -46.770 |
| 31 - 34° | 1059.41 | 939.54 | 1706.04 | -4.158 | 26.561 |
| 34 - 37° | 73.75 | 54.44 | 809.81 | -0.670 | 26.190 |
| > 37° | 12.23 | 2.04 | 6.91 | -0.354 | 0.169 |
| Total = | 2742.75 | 2742.76 | 2744.12 | | |

**Source: Researcher's Analysis, 2024** **Δ** Percentage Change

To give a clearer understanding of the temperature variance at various LST ranges, percentage change in LST was used. Whereas, the categorised LST for 2003 showed that a greater percentage of the region had surface temperatures between 28° and 31°C and 31° and 34°C, respectively, covering 52.77% and 36.75% of the entire study area. Only 7.44% and 0.054% of the entire land surface recorded temperatures between 25° and 28°C and less than 25°C, respectively. Hence, LST greater than 37°C was identified to cover 0.42% of the total area of study for the year 2003. In 2013, LST within the range of 28º - 31ºC and 31º - 34ºC accounted for 57.47% and 32.59 spatial

extent of the study area respectively. Only 7.94% and 0.041% of the spatial trend is within the range of 25º -28ºC and <25ºC. Consequently, LST identified to be within 34º -37ºC represented 1.89% and greater than >37ºC is 0.071% of the spatial trend. From 2023, LST is within the range of 31º-34ºC which accounted for 59.15% and 34º -37ºC which constituted 28.08% of the study area respectively. The higher LST dominates northwestern and north central areas of the city, while the eastern, southern and extreme northern areas have the lower LST. The UHI impacts of built-up areas were found to depend on the density of settlement with medium sized building. In Abuja city, settlements in the south of the city are less populated and have visible green spaces as compared with areas to the north. The results verify a previous Abuja UHI projected (Adeyeri *et al*, 2015) which reported a consistent high UHI intensity in northwestern Abuja city area as compared to the east and downtown area.

**Analysis of Urban Heat Islands (UHI)**

The UHI map in Figure 2,3 and 4 below shows a clear depiction of UHI intensity across the AMAC, categorized into five distinct temperature ranges. These ranges from 0 – 1.67°C (blue), 1.68 – 1.93°C (light blue), 1.94 – 2.12°C (green), 2.13 – 2.31°C (yellow), and 2.32 – 4.78°C (red), with the colours indicating varying levels of heat intensity.

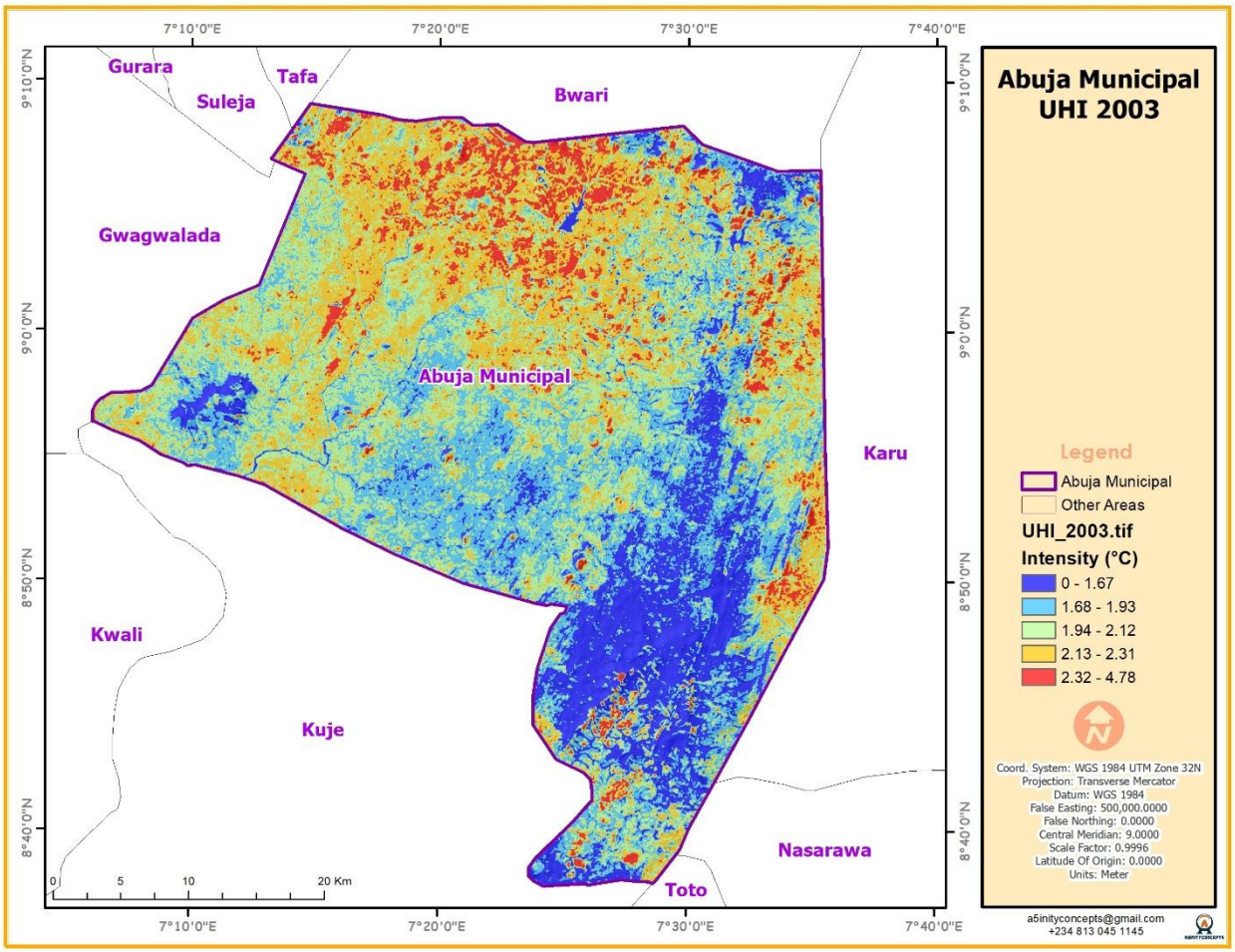


**Figure 2: Urban Heat Intensity of Abuja Metropolis for 2003.**

The UHI map of AMAC for 2003 as seen in figure 2 above shows that Central Business District and other districts such as Wuse, Garki, and Maitama, known for their dense commercial and residential developments, are the primary contributors to higher UHI intensity. Wuse, being one of the most commercial and densely populated districts, and Garki, known for government offices and dense residential areas, shows significant UHI effects. Maitama, while affluent and developed, still maintains some green spaces but not enough to mitigate the high UHI effects fully. Moving to the northern suburbs, districts like Gwarinpa, with its large residential estates, Jabi and Utako, which have a mix of commercial and residential developments, exhibit moderate to high UHI intensities. On the other hand, the southern outskirts of Abuja, including Karu and Nyanya, show lower UHI intensities, likely due to less urbanization at the time. Similarly, the northern outskirts3, including Katampe and Jahi, are less developed and have more vegetation, contributing to lower UHI effects.

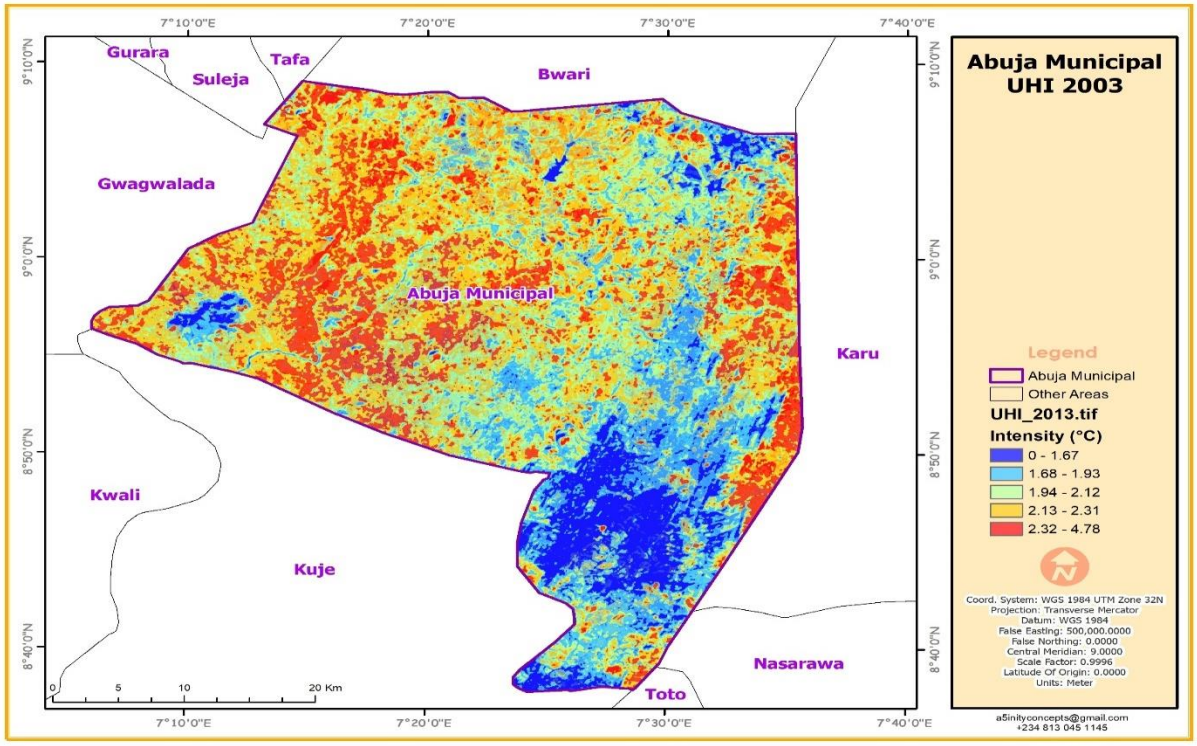


**Figure 3: Urban Heat Intensity of Abuja Metropolis for 2013.**

The 2013 UHI map as seen in figure 3 above shows that high-intensity UHI zones, indicated in red, are prominently found in central districts such as Wuse, Garki, and Maitama. These areas had high UHI in 2003 and continues to exhibit high UHI intensities due to their dense commercial and residential developments, extensive urbanization, and limited green spaces. Additionally, districts like Jabi, Utako, and Gwarinpa also show high UHI intensities. Gwarinpa, known for its large residential estates, Jabi and Utako, with their mix of commercial and residential developments, have experienced increased urbanization, contributing to higher UHI effects. Moderate-intensity UHI zones in 2013 are found in areas surrounding the high-intensity zones, including parts of the northern and western suburbs. These zones have undergone urban growth but still retain some

green spaces, which help mitigate the UHI effect to a certain extent. Low-intensity UHI zones, depicted are located on the outskirts of Abuja, particularly in the southern regions such as Karu and Nyanya, and northern suburbs like Kubwa and Dutse. These areas have less urban development and more vegetation, resulting in cooler temperatures. Similarly, the southwestern regions near Kuje and the areas bordering Kwali show low UHI effects, indicating lesser urbanization and higher vegetation cover.

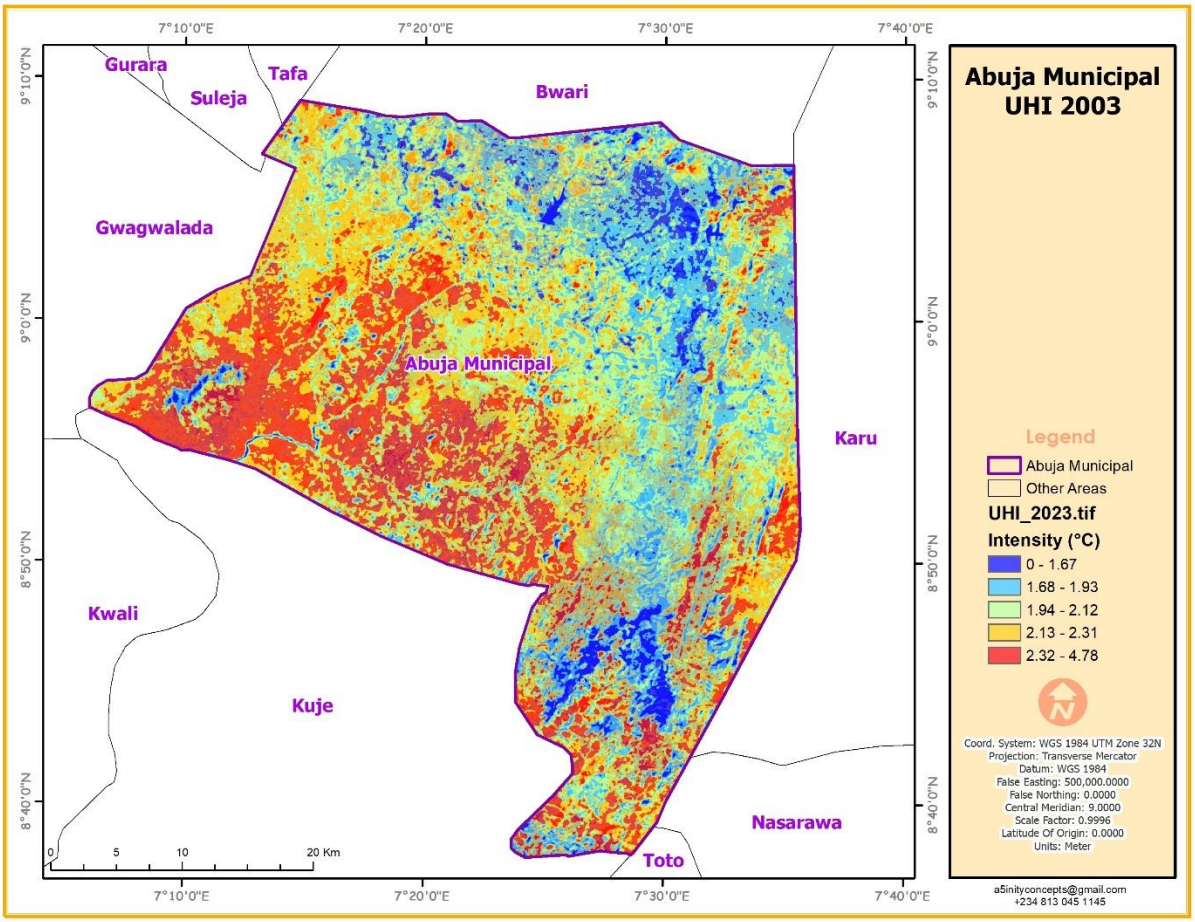


**Figure 4: Urban Heat Intensity of Abuja Metropolis for 2023**

In figure 4, the UHI of Abuja metropolis for 202 3 shows that the central districts, including Wuse, Garki, and Maitama, continue to be major hotspots for high UHI intensity. These areas remain densely populated and highly developed, with extensive commercial and residential structures contributing to significant heat retention. The increased urbanization in these regions is evident, as indicated by the pervasive red zones on the map, signifying the highest UHI intensities (from 0.62 to 0.975 °C). Furthermore, the districts of Jabi, Utako, and Gwarinpa also display high UHI intensities, similar to observations in 2013. Gwarinpa's large residential estates and the mixed commercial-residential developments in Jabi and Utako have seen further urban growth, resulting in increased heat retention. The persistence and expansion of these high-intensity zones emphases the cumulative impact of urbanization on UHI effects over time. In terms of moderate UHI intensity zones (0.391 to 0.619 °C), areas surrounding the central districts and extending towards the northern and western suburbs exhibit noticeable UHI effects. The outskirts of Abuja

Metropolis, particularly the southern regions such as Karu and Nyanya, along with northern suburbs like Kubwa and Dutse, display lower UHI intensities, indicated by the blue and light blue areas on the map. These regions have less urban development and more vegetation, contributing to cooler temperatures. Notably, the southwestern areas near Kuje and bordering Gwagwalada continue to exhibit low UHI effects, reflecting limited urbanization and significant green cover. The finding is in tandem with the result of United Nations Population Fund cited by Agu, Ikwuka and Hudu (2021) which states that "more than fifty percent of the world's population lives in cities and this ratio projected to increase".

The comparative scrutiny reveals several trends and shifts in UHI patterns over the years. The central districts, consistently high in UHI intensity since 2003, have seen an increase in urban density and heat retention, as indicated by the sustained red zone as seen in figure 2,3 and 4 above. In the northern suburbs, districts like Gwarinpa, Jabi, and Utako have shown a marked increase in UHI intensity compared to 2013, indicating substantial urban development over the past decade. This trend highlights the ongoing expansion and its impact on UHI effects, with these areas becoming more urbanized and less vegetated over time. Conversely, the southern outskirts, including Karu and Nyanya, have maintained lower UHI intensities, similar to previous years. These areas have not experienced the same level of urban growth as the central and northern districts, retaining more natural landscapes and vegetation, which contribute to cooler temperatures. The southwestern regions near Kuje continue to exhibit low UHI effects, reinforcing the importance of green spaces in mitigating urban heat.

The result is in line with Isioye *et al* (2020) findings on urban intensity's impact of UHI patterns on the relationship between urban development and heat retention. They found that increased urban density leads to a rise in local temperatures due to a decrease in natural landscapes and vegetation. Consequently, Ammar (2021) emphasized the cooling effect of green spaces, suggesting that the presence of vegetation significantly reduces UHI effects. Additionally, Awuh *et al* (2021) and Agu *et al* (2021) discusses how urban expansion, especially in previously vegetated areas, exacerbates UHI effects, as seen in the northern suburbs. This study emphasizes the crucial role of urban planning and green spaces in managing UHI.

## Conclusion

This study adopted geospatial techniques in assessing the spatiotemporal variation of the surface urban heat intensity in Abuja Municipal Area Council, FCT from 2003 to 2023.The result reveals that the highest UHI intensities from 2.32 to 4.76 °C, moderate UHI intensity zones 1.94 to 2.31 °C and lower intensity 1. 07 to 1.93 °C respectively, thus, indicating the presence of a strong urban heat island.

UHIs is a bad trend for AMAC because it is a factor contributing to the microclimatic warming that is currently occurring in the study area; if nothing is done to mitigate this trend in UHI intensification, the study area may experience severe UHI, which will have a negative impact on AMAC livelihoods. The outcome of the study reaffirms the efficiency and capability of Remote sensing technique in considering various parameters for the complex and dynamic real-world datasets.

## Recommendations

Based on the findings, the following recommendations are made:

i. The paper recommends that, Urban planners and local administrators should emphasize sustainable urban development that will reduce the effect of UHI and encourage the establishment of parks and open space to serve as shelter-belt for ecological stability.
ii. The author strongly suggests that the main solution to deforestation and urbanization has to start from local action where the local inhabitants will be educated on the need for sustainable city.
iii. Planting of the loss native trees and protection of existing vegetation from fire and land clearing should also be encouraged, as the restoration of degraded lands and stabilization of ecosystem for combating climate variability or change.
iv. Since effectiveness of a surface in reducing daytime urban air temperatures depends strongly on the amount of heating avoided, the study recommends preserving and replicating greenery, light colored facades as measures to reduce the effects of urban heat island.

## Reference

Adebayo, F.F., Balogun, I.A, Adediji, A.T., Akande, O. & Abdulkareem, S.B. (2017). Assessment of Urban Heat Island over Ibadan Metropolis Using Landsat and Modis. *International Journal of Environment and Bioenergy, 12(1): 62-87.*

Adeyeri, O.E., Okogbue, E.C, Ige, S.O. & Ishola, K.A. (2015). Estimating the Land Surface Temperature over Abuja using Different Landsat sensors in Proceedings of Climate Change, Environmental Challenges and Sustainable Development pp. *305-310.*

Adakayi, P.E. (2000). 'Climate'. In: Dawam P.D. (Ed) Geography of Abuja: Federal Capital Territory. Famous/Asanlu Publishers, Abuja.

Adinna, E.N., Enete, I.C. & Arch, T.O. (2009) Assessment of Urban Heat Island and Possible Adaptations in Enugu Urban Using Landsat-ETM. *Journal of Geography and Regional Planning, 2(2), 030-036.*

Ahmed, B., Kamruzzaman, M., Zhu, X., Rahman, M.S. & Choi, K. (2013). Simulating Land Cover Changes and their Impacts on Land Surface Temperature in Dhaka, Bangladesh, *Rem. Sens. 5 5969–5998.*

Aghamohammadi, N., Ramakreshnan, L., Fong, C.S. & Sulaiman, N.M. (2021). Urban Heat Island, Contributing Factors, Public Responses and Mitigation Approaches in the Tropical Context of Malaysia. U*rban Heat Island Mitigat. 2021, 107–121.*

Agu, C.C., Ikwuka, A. & Hudu, H.M. (2021) Environmental Impact Analysis on the Increase in Temperature and Urban Heat Island: A Case Study of Gwagwalada, Abuja. *Journal of Oceanography and Marine Research S4: 006. Pp 1-7.*

Alfraihat, R., Mulugeta, G. & Gala, T. S. (2016). Ecological Evaluation of Urban Heat Island in Chicago City, USA. *Journal of Atmospheric Pollution, 4(1): 23-29.*

Ammar, A. (2021). Analysis of Urban Heat Island Characteristics and Mitigation Strategies for Eight Arid and Semi-Arid Gulf Region Cities. *Environmental Earth Sciences 80:258-259.*

Archisman, B., Sunny, K., Praveen, K. & Parth P.S. (2017). "Characteristics of Surface Urban Heat Island (SUHI) over the Gangetic Plain of Bihar, India". Centre for Environmental Sciences, Central University of South Bihar, Bihar, India. Asia-Pac. *J. Atmos. Sci., 54(2), 205-214.*

Ashley, M. (2016). "Assessing The Urban Heat Island of a Small Urban Area in Central Pennsylvania Along the Susquehanna River". *Department of Geography and Earth Science and the Graduate Council,* Shippensburg University. Shippensburg, Pennsylvania.

Awuh, M.E., Japhet's, P.O. & Enete, I.C. (2021*)* Geospatial Techniques, a Superlative Method to Assess Urban Heat Island Intensity: The Case of Abuja Municipal, Nigeria. *Journal of Geographic Information System, 13, 52-64.*

Ayanlade, A., Aigbiremolen, M.I. & Oladosu, O.R. (2021). Variations in Urban Land Surface Temperature Intensity over Four Cities in Different Ecological Zones. *Journal of Scientific Report 11: 20537*

Balogun, O. (2001). *The Federal Capital Territory of Nigeria: Geography of Its Development*. University Press, Ibadan.

Congalton, R. & Green, K. (2008). *Assessing the Accuracy of Remotely Sensed Data: Principles and Practices.* Second Edition, CRC Press Boca Raton.

Good, T. & Giordano, P. A. (2019). *Methods for Constructing a Color Composite Image*. In: Google Patents.

Hammada, M., Mucsi, L. & Van-Leeuwen, B. (2018). Land Cover Change Investigation in the Southern Syrian Coastal Basin during the Past 30-years Using Landsat Remote Sensing Data. *Journal of Environmental Geography*11(2) 45-51

Isioye, O. A., Ikwueze, H. U. & Akomolafe, E. A. (2020) Urban Heat Island Effects and Thermal Comfort in Abuja Municipal Area Council of Nigeria. *FUTY Journal of the Environment 14(2), 19-34.*

Khaled, A., Adeline, N., Ahmed, D., Mahmoud, A., Sayed, A. & Fathi, A. (2015). Assessment of Urban Heat Island Using Remotely Sensed Imagery over Greater Cairo, Egypt. *Advances in Remote Sensing, 2015, 4, 35-47.*

Liu, L. & Zhang, Y. (2011). Urban Heat Island Analysis Using the Landsat TM Data and ASTER Data: A Case Study in Hong Kong. *Remote Sensing, 3(7), 1535-1552.*

Mande, K.H. & Abashiya, D.O. (2020). Assessment of Urban Heat Island in Kaduna Metropolis Between 2000 and 2018. *FUDMA Journal of Sciences (FJS), 4(4), 166 – 174.*

Meenal, S. & Rajashree, K. (2017). "Assessment of Urban Heat Island through Remote Sensing in Nagpur Urban Area Using Landsat 7 ETM+ Satellite Images". *World Academy of Science, Engineering and Technology International Journal of Urban and Civil Engineering*, 11(7).

Mondal, M. S., Sharma, N., Garg, P.K. & Kappas, M. (2016) 'Statistical Independence Test and Validation of CA Markov LULC Prediction Results', *The Egyptian Journal of Remote Sensing and Space Science, 19(2), 259–272.*

Muhammad, I., Abubakar, S. & Shehu, Y. (2013). Spatial Analysis of Urban Growth in Kazaure Local Government Area of Jigawa State, Nigeria. *International Journal of Geomatics and Geosciences, 4(1), 22.*

Nguyen, T. H., Yuei-An, L., Kim-Anh, N., Ram, C. S., Duy-Phien, T., Chia-Ling, L. & Dao, D. C. (2018). "Assessing the Effects of Land-Use Types in Surface Urban Heat Islands for Developing Comfortable Living in Hanoi City".

Nkeki, F.N. & Ojeh, V.N. (2014). Flood risks analysis in a littoral African city: Using geographic information system. In: Geographic Information Systems (GIS): Techniques, Applications and Technologies. Nielson D (Editor), Nova Science Publishers, *New York, USA, pp.:279-316.*

Oyinloye, M.A. (2013). Geospatial Analysis of Urban Growth in Akure, Ondo State, Nigeria. *American Journal of Social Issues and Humanities* 3 (4), 200-212

Pontius Jr, R.G. & Millones, M. (2011). Death to Kappa: Birth of Quantity Disagreement and Allocation Disagreement for Accuracy Assessment. *International Journal of Remote Sensing, 32(15), 4407-4429.*

Rahman, M., Aldosary, A. S. & Mortoja, M. (2017). Modeling Future Land Cover Changes and their Effects on the LST in the Saudi Arabian Eastern Coastal City of Dammam. *Land, 6(2), 36.*

Sholihah, R. I. & Shibata, S. (2019). *Retrieving Spatial Variation of Land Surface Temperature Based on Landsat OLI/TIRS of Southern Jember, Java, Indonesia.* Paper presented at the IOP Conference Series: Earth and Environmental Science.

Thomas, U.O. (2020). Ecological Evaluation of Urban Heat Island Impacts in Abuja Municipal Area of FCT Abuja, Nigeria. *World Academics Journal of Engineering Sciences, 7(1), 66-72.*

United Nation Development Programme (UNDP)(2022). *Human Development Report 2021/2022, Uncertain times, Unsettled lives:* Shaping our future in a Transforming World UN Plaza, New York USA

World Urbanization Prospects (2019). *United Nations Department of Economic and Social Affairs/Population Division.* Department of Economic and Social Affairs Population Division

Zine El Abidine, E. M., Mohieldeen, Y. E., Mohamed, A.A., Modawi, O. & Al-Sulaiti, M.H. (2014). Heat Wave Hazard Modelling: Qatar Case Study. *QScience connect, 9.*